Table 3. *Refined values of the mosaic spread (full width at half height in seconds of arc) as obtained from monochromatic and TOF neutrons for model Z*

	MON	TOF
15 K	3·8 (1)	8·1 (3)
60 K	3·2 (1)	10·2 (3)
295 K	4·0 (1)	12·4 (4)

extinction is pronounced only for few reflections which leads to refined mosaic spreads that are considerably smaller than the experimental estimates. It thus appears that the extinction corrections will be overestimated in least-squares refinements that are based on data sets where only a small part of the reflections are affected by extinction.

The overall counting statistical precision of a data set may be summarized by the statistical R factor, $R_{stat}(F^2) = \sum\sigma_{cs}(F^2)/\sum F^2$, which imposes a lower limit to the conventional crystallographic R factor, $R(F^2) = \sum|F^2_{obs} - F^2_{calc}|/\sum F^2_{obs}$. It is apparent from Table 1 that the TOF data are subject to additional uncertainties besides counting statistics to a higher degree than the monochromatic data. The agreement of the derived results, however, indicates these additional uncertainties to be of a random rather than of a systematic nature.

The purpose behind the measurement of data sets with two methods was to check whether the mean thermal nuclear positions of fluorine differ in the paramagnetic and antiferromagnetically ordered state. Actually, the low temperature of the neutron investigation reported in I as 15 K was about 60 K. We now find that at 15 K, the magnetostrictive shifts $\Delta x = x(15\text{ K}) - x(295\text{ K})$ are $-2{\cdot}9\,(4) \times 10^{-4}$ and $-2{\cdot}7\,(4) \times 10^{-4}$ using monochromatic and TOF neutrons, respectively. This corresponds to an average shift of $1{\cdot}95\,(20) \times 10^{-3}$ Å in the Mn—F distance within the plane normal to the c axis. This shift is different from the result deduced from γ-ray diffraction: $\Delta x = -4{\cdot}8\,(7) \times 10^{-4}$. The implications of this subtle difference will be discussed in a forthcoming paper, dealing with the charge density distribution in MnF_2.

The work at Argonne was supported by the Office of Basic Energy Sciences, Division of Materials Sciences, US Department of Energy, under contract W-31-109-Eng-38.

References

BECKER, P. J. & COPPENS, P. (1974). *Acta Cryst.* A**30**, 129–147.

BUSING, W. R., MARTIN, K. O. & LEVY, H. A. (1962). *ORFLS*. Report ORNL-TM-305. Oak Ridge National Laboratory, Tennessee, USA.

HAEFNER, K. (1964). Thesis, Univ. of Chicago, USA.

HALL, S. R. & STEWART, J. M. (1989). Editors. *XTAL2.6 User's Manual*. Univs. of Western Australia, Australia, and Maryland, USA.

JAUCH, W., SCHULTZ, A. J. & SCHNEIDER, J. R. (1988). *J. Appl. Cryst.* **21**, 975–979.

LEHMANN, M. S., KUHS, W. F., MCINTYRE, G. J., WILKINSON, C. & ALLIBON, J. R. (1989). *J. Appl. Cryst.* **22**, 562–568.

SCHERINGER, C. (1986). *Acta Cryst.* A**42**, 356–362.

WILKINSON, C., KHAMIS, H. W., STANSFIELD, R. F. D. & MCINTYRE, G. J. (1988). *J. Appl. Cryst.* **21**, 471–478.

ZACHARIASEN, W. H. (1967). *Acta Cryst.* **23**, 558–564.

ZUCKER, U. H., PERENTHALER, E., KUHS, W. F., BACHMANN, R. & SCHULZ, H. (1983). *J. Appl. Cryst.* **16**, 358.

ZUCKER, U. & SCHULZ, H. (1982). *Acta Cryst.* A**38**, 563–568.

Acta Cryst. (1990). B**46**, 742–747

Structures of $Na(In,Sc)Si_2O_6$ Clinopyroxenes Formed at 6 GPa Pressure

BY HARUO OHASHI, TOSHIKAZU OSAWA AND AKIRA SATO

National Institute for Research in Inorganic Materials, Namiki 1-1, *Tsukuba, Ibaraki* 305, *Japan*

(*Received* 4 *January* 1990; *accepted* 12 *July* 1990)

Abstract

Crystal structures have been refined from single-crystal X-ray data for nine synthetic clinopyroxenes in the system $NaInSi_2O_6$–$NaScSi_2O_6$, crystallized at 1770 K and 6 GPa pressure. The structures are isomorphous with other sodium pyroxenes. The space group is $C2/c$, $Z = 4$. In and Sc occupy a distorted octahedral ($M1$) site. The $M1$—$M1$ distances and the $M1$—O1—$M1$ angles correlate with the mean $M1$—O1 distances in such a way as to follow two different trends, suggesting that there are two different electronic states for the octahedral In^{3+} ions. The Si—O distances constitute two populations which can be related to the mean electronegativity of the octahedral ($M1$) ions. From the Si—O distances, the electronegativites of the two In^{3+} ions are 1·2 and 1·7 on Pauling's scale.

0108-7681/90/060742-06$03.00

Table 1. *Crystal data for nine* $Na(In,Sc)Si_2O_6$ *clinopyroxenes*

	In100	In80Sc20	In65Sc35	In60Sc40	In55Sc45	In50Sc50	In40Sc60A*	In40Sc60	In20Sc80
a (Å)	9·8997 (5)	9·8907 (5)	9·8811 (5)	9·8782 (5)	9·8734 (5)	9·8701 (4)	9·8634 (6)	9·8659 (5)	9·8516 (5)
b (Å)	9·1310 (3)	9·1164 (2)	9·1043 (2)	9·1008 (3)	9·0947 (2)	9·0901 (2)	9·0827 (3)	9·0848 (2)	9·0698 (2)
c (Å)	5·3656 (3)	5·3623 (3)	5·3592 (3)	5·3582 (3)	5·3570 (3)	5·3559 (2)	5·3542 (4)	5·3553 (3)	5·3521 (3)
β (°)	107·226 (2)	107·204 (2)	107·188 (2)	107·191 (2)	107·187 (2)	107·179 (2)	107·174 (3)	107·178 (2)	107·175 (2)
V (Å^3)	463·26 (4)	461·87 (4)	460·59 (4)	460·18 (4)	459·55 (4)	459·10 (3)	458·28 (5)	458·58 (3)	456·90 (3)
M_r	289·98	276·00	265·52	262·03	258·54	255·04	248·06	248·06	234·08
D_x (g cm^{-3})	4·16	3·97	3·83	3·78	3·74	3·69	3·59	3·59	3·40

* Annealed at 1073 K and atmospheric pressure.

Table 2. *Data collection information for nine* $Na(In,Sc)Si_2O_6$ *clinopyroxenes*

	In100	In80Sc20	In65Sc35	In60Sc40	In55Sc45	In50Sc50	In40Sc60A	In40Sc60	In20Sc80
Size of crystal (mm)	0·13 × 0·06 × 0·08	0·13 × 0·12 × 0·12	0·08 × 0·08 × 0·06	0·11 × 0·08 × 0·04	0·16 × 0·12 × 0·11	0·12 × 0·08 × 0·06	0·12 × 0·12 × 0·12	0·12 × 0·12 × 0·12	0·17 × 0·10 × 0·10
μ (cm^{-1})	55·8	49·0	44·0	42·3	40·6	38·9	35·5	35·5	28·6
F (000)	544	521·6	504·8	499·2	493·6	488·0	476·8	476·8	454·4
T (K)	296	297	297	296	296	296	297	298	298
h	0 to 14	0 to 14	0 to 14	0 to 14	0 to 14	0 to 14	0 to 14	0 to 14	0 to 14
k	0 to 13	0 to 13	0 to 13	0 to 13	0 to 13	0 to 13	0 to 13	0 to 13	0 to 13
l	−7 to 7	−7 to 7	−7 to 7	−7 to 7	−7 to 7	−7 to 7	−7 to 7	−7 to 7	−7 to 7
No. of reflections									
Measured	807	805	802	802	801	801	800	800	798
Observed	793	800	776	761	790	767	785	790	781
Used	792	799	774	758	787	759	771	785	780
R	1·671	1·857	1·654	2·011	1·887	2·351	1·839	1·818	1·938
wR	3·745	4·641	3·158	3·172	5·128	4·351	4·344	4·255	5·560
S	1·674	2·146	1·370	1·368	2·330	1·894	1·977	1·933	2·490
$(\Delta/\rho)_{max}$ (e Å^{-3})	0·719	0·851	0·834	0·749	0·700	0·824	0·618	0·605	0·585
$(\Delta/\rho)_{min}$ (e Å^{-3})	−0·652	−1·243	−0·841	−1·458	−1·027	−0·991	−0·695	−0·889	−1·210

Introduction

The dependence of Si—O distance on the size and electronegativity of the octahedral M^{3+} ion was examined for the $NaM^{3+}Si_2O_6$ pyroxenes by Ohashi (1979, 1981, 1983) and Ohashi, Fujita & Osawa (1982, 1983). The Si—O distances correlate with the electronegativities of the octahedral ($M1$) ions in such a way that they follow two different trends: the Sc–Ti–V–Cr–Al series and the In–Fe–Ga series. In the former, the octahedral ($M1$) sites are occupied by lower electron density ions, whereas in the latter the octahedral ($M1$) sites are occupied by higher electron density ions. To study the role of the mean electron density of the octahedral ($M1$) ions, the crystal structures have been refined for nine synthetic clinopyroxenes in the system $NaInSi_2O_6$–$NaScSi_2O_6$.

Experimental

All the crystals were synthesized by solid-state reaction using a belt-type high-pressure apparatus (Fukunaga, Yamaoka, Endo, Akaishi & Kanda, 1979). Mixtures of crystalline $Na_2Si_2O_5$, In_2O_3, Sc_2O_3 and SiO_2 were sealed in platinum capsules and maintained at 1770 K and 6 GPa for 20 h. Unit-cell dimensions of the resulting clinopyroxenes were determined from 2θ values of 25 reflections in the range $55 < 2\theta < 65°$, measured on a four-circle diffractometer with Mo $K\alpha_1$ ($\lambda = 0{\cdot}70930$ Å) (Table 1). The chemical compositions of the pyroxenes were determined by microprobe analysis using $NaInSi_2O_6$ pyroxene and $Sc_2Si_2O_7$ thortveitite as standards, and by interpolation of the unit-cell dimensions. After the intensity data collection, $Na(In_{0{\cdot}40}Sc_{0{\cdot}60})Si_2O_6$ pyroxene was annealed by heating at 1073 K and atmospheric pressure for 70 h, and intensity data were recollected; this pyroxene is labelled In40Sc60A in the tables.*

The intensity measurements at room temperature were made with an Enraf–Nonius CAD-4 diffractometer using graphite-monochromatized Mo $K\alpha$ ($\lambda = 0{\cdot}71073$ Å) radiation. Information on data collection is summarized in Table 2. The intensities of the reflections were collected in the range $2\theta < 63°$ using variable-rate ω–2θ scans with scan range $(0{\cdot}8 + 0{\cdot}35\tan\theta)°$. The observed intensities were corrected for Lorentz, polarization and monochromator-polarization factors. No absorption corrections were applied although extinction corrections were made. The least-squares refinements were based on F_o values greater than $3\sigma(F_o)$. The structure refinements were carried out on a MicroVAXII computer, using Enraf–Nonius (1985) *SDP* programs. Initial positional parameters and isotropic displacement factors were those of $NaScSi_2O_6$ (Hawthorne & Grundy,

* Lists of structure factors, atomic coordinates and anisotropic thermal parameters have been deposited with the British Library Document Supply Centre as Supplementary Publication No. SUP 53425 (54 pp.). Copies may be obtained through The Technical Editor, International Union of Crystallography, 5 Abbey Square, Chester CH1 2HU, England.

Table 3. *Fractional atomic coordinates and equivalent isotropic displacement parameters* (Å^2) *for nine* $Na(In,Sc)Si_2O_6$ *clinopyroxenes*

$B_{eq} = (4/3)\sum_i\sum_j \beta_{ij}\mathbf{a}_i.\mathbf{a}_j$.

		In100	In80Sc20	In65Sc35	In60Sc40	In55Sc45	In50Sc50	In40Sc60A	In40Sc60	In20Sc80
Si	x	0·29172 (7)	0·29169 (7)	0·29162 (5)	0·29160 (5)	0·29152 (6)	0·29153 (6)	0·29145 (5)	0·29135 (4)	0·29117 (5)
	y	0·08660 (6)	0·08661 (6)	0·08678 (5)	0·08680 (5)	0·08682 (6)	0·08684 (6)	0·08692 (5)	0·08695 (4)	0·08721 (5)
	z	0·2475 (1)	0·2472 (1)	0·24646 (9)	0·2463 (1)	0·2461 (1)	0·2460 (1)	0·24583 (8)	0·24575 (8)	0·24473 (9)
	B	0·412 (9)	0·395 (8)	0·390 (6)	0·423 (7)	0·345 (7)	0·321 (8)	0·328 (6)	0·343 (5)	0·336 (6)
O1	x	0·1190 (2)	0·1191 (2)	0·1190 (1)	0·1188 (1)	0·1190 (1)	0·1188 (2)	0·1189 (1)	0·1193 (1)	0·1187 (1)
	y	0·0797 (2)	0·0792 (2)	0·0789 (1)	0·0790 (1)	0·0788 (2)	0·0789 (2)	0·0789 (1)	0·0794 (1)	0·0786 (1)
	z	0·1505 (3)	0·1495 (3)	0·1496 (2)	0·1489 (2)	0·1489 (3)	0·1486 (3)	0·1478 (2)	0·1482 (2)	0·1476 (2)
	B	0·53 (2)	0·53 (2)	0·53 (2)	0·55 (2)	0·51 (2)	0·47 (2)	0·45 (2)	0·45 (2)	0·46 (2)
O2	x	0·3568 (2)	0·3570 (1)	0·3577 (1)	0·3576 (1)	0·3577 (2)	0·3581 (2)	0·3583 (1)	0·3583 (1)	0·3588 (1)
	y	0·2455 (2)	0·2464 (2)	0·2464 (1)	0·2465 (1)	0·2470 (2)	0·2468 (2)	0·2466 (1)	0·2463 (1)	0·2470 (1)
	z	0·3177 (3)	0·3152 (3)	0·3140 (2)	0·3138 (2)	0·3131 (3)	0·3121 (3)	0·3119 (2)	0·3117 (2)	0·3094 (2)
	B	0·75 (2)	0·74 (2)	0·72 (2)	0·75 (2)	0·70 (2)	0·67 (2)	0·68 (2)	0·70 (2)	0·65 (2)
O3	x	0·3488 (1)	0·3491 (1)	0·3494 (1)	0·3494 (1)	0·3500 (1)	0·3497 (1)	0·3497 (1)	0·34975 (9)	0·3500 (1)
	y	0·0115 (2)	0·0111 (2)	0·0107 (1)	0·0105 (2)	0·0101 (2)	0·0100 (2)	0·0096 (2)	0·0093 (1)	0·0089 (2)
	z	0·0172 (3)	0·0182 (3)	0·0186 (2)	0·0182 (2)	0·0186 (2)	0·0187 (2)	0·0177 (2)	0·0180 (2)	0·0187 (2)
	B	0·66 (2)	0·67 (2)	0·63 (2)	0·67 (2)	0·60 (2)	0·57 (2)	0·61 (2)	0·61 (2)	0·58 (2)
*M*1(In,Sc)	y	0·89471 (2)	0·89485 (2)	0·89507 (2)	0·89511 (2)	0·89518 (2)	0·89525 (3)	0·89535 (2)	0·89536 (2)	0·89571 (3)
	B	0·417 (4)	0·397 (4)	0·418 (3)	0·413 (3)	0·410 (5)	0·411 (5)	0·377 (4)	0·403 (4)	0·430 (5)
*M*2(Na)	y	0·3033 (2)	0·3036 (1)	0·3039 (1)	0·3037 (1)	0·3037 (1)	0·3038 (2)	0·3036 (1)	0·3039 (1)	0·3039 (1)
	B	1·47 (3)	1·40 (2)	1·36 (2)	1·42 (2)	1·35 (2)	1·25 (2)	1·30 (2)	1·33 (2)	1·27 (2)

Table 4. *M*1(In,Sc)—O *and* *M*1—*M*1 *distances* (Å), *M*1—O1—*M*1 *angles* (°), Si—O *distances* (Å), *and* Si—O3—Si *and* O3—O3—O3 *angles* (°) *in* $Na(In,Sc)Si_2O_6$ *pyroxenes*

	*M*1—O1*A*1,*B*1	*M*1—O1*A*2,*B*2	*M*1—O2*C*1,*D*1	⟨*M*1—O1⟩	*M*1—*M*1	*M*1—O1—*M*1
In100	2·213 (2)	2·136 (1)	2·074 (2)	2·174	3·3007 (1)	98·74 (6)
In80Sc20	2·209 (2)	2·131 (1)	2·061 (2)	2·170	3·2961 (1)	98·84 (5)
In65Sc35	2·202 (1)	2·130 (1)	2·053 (1)	2·166	3·2910 (1)	98·88 (4)
In60Sc40	2·202 (1)	2·126 (1)	2·052 (1)	2·164	3·2898 (2)	98·95 (5)
In55Sc45	2·199 (2)	2·126 (1)	2·045 (2)	2·163	3·2878 (2)	98·95 (5)
In50Sc50	2·199 (2)	2·123 (1)	2·042 (2)	2·161	3·2860 (2)	98·96 (6)
In40Sc60A	2·198 (1)	2·119 (1)	2·040 (1)	2·159	3·2834 (2)	99·01 (4)
In40Sc60	2·204 (1)	2·122 (1)	2·042 (1)	2·163	3·2840 (2)	98·77 (4)
In20Sc80	2·191 (1)	2·117 (1)	2·029 (1)	2·154	3·2772 (1)	99·05 (4)
Sc100*	2·183 (2)	2·105 (5)	2·017 (2)	2·144	3·269 (1)	99·3 (1)

	Si—O(1)	Si—O(2)	⟨Si—O(nbr)⟩	Si—O(3)	Si—O(3)	⟨Si—O(br)⟩	⟨Si—O⟩
In100	1·634 (2)	1·587 (2)	1·611	1·653 (2)	1·653 (2)	1·653	1·632
In80Sc20	1·632 (2)	1·591 (2)	1·612	1·648 (2)	1·655 (1)	1·652	1·632
In65Sc35	1·631 (1)	1·590 (1)	1·611	1·645 (1)	1·658 (1)	1·652	1·631
In60Sc40	1·632 (1)	1·590 (1)	1·611	1·648 (1)	1·655 (1)	1·652	1·631
In55Sc45	1·629 (2)	1·594 (2)	1·612	1·650 (2)	1·656 (1)	1·653	1·632
In50Sc50	1·630 (2)	1·592 (2)	1·611	1·647 (2)	1·656 (1)	1·651	1·631
In40Sc60A	1·628 (1)	1·589 (1)	1·609	1·652 (1)	1·651 (1)	1·651	1·630
In40Sc60	1·623 (1)	1·587 (1)	1·605	1·653 (1)	1·651 (1)	1·652	1·629
In20Sc80	1·625 (1)	1·590 (1)	1·608	1·649 (1)	1·656 (1)	1·652	1·630
Sc100*	1·630 (3)	1·592 (2)	1·611	1·653 (2)	1·653 (3)	1·653	1·632

	Si—O3—Si	O3—O3—O3		Si—O3—Si	O3—O3—O3
In100	140·84 (10)	171·03 (8)	In50Sc50	140·52 (9)	172·20 (9)
In80Sc20	140·76 (9)	171·40 (7)	In40Sc60A	140·46 (7)	172·52 (7)
In65Sc35	140·66 (7)	171·65 (7)	In40Sc60	140·43 (6)	172·79 (6)
In60Sc40	140·62 (8)	171·86 (7)	In20Sc80	140·32 (7)	173·10 (8)
In55Sc45	140·31 (9)	172·16 (7)	Sc100*	140·2 (1)	173·6 (1)

* Hawthorne & Grundy (1973).

1973). The atomic scattering factors (including f' and f'') for neutral atoms were taken from *International Tables for X-ray Crystallography* (1974, Vol. IV).

Final unweighted R and weighted $[1/\sigma(F)]^2$ R indices are listed in Table 2, all $(\Delta/\sigma)_{max} = 0{\cdot}00$, and final parameters are listed in Table 3. The atomic coordinates of the $NaInSi_2O_6$ pyroxene formed at 6 GPa pressure are in good agreement with those of the $NaInSi_2O_6$ pyroxene formed at atmospheric pressure (Hawthorne & Grundy, 1974). Bond lengths and angles are listed in Table 4, together with the published values for $NaScSi_2O_6$ (Hawthorne & Grundy, 1973).

Description and discussion

*M*1 octahedron

$Na(In,Sc)Si_2O_6$ pyroxenes are isomorphous with other Na pyroxenes (Clark, Appleman & Papike, 1969). In and Sc occupy a distorted octahedral (*M*1) site. The variations in the mean *M*1—O1 (hereafter abbreviated ⟨*M*1—O1⟩) and *M*1—*M*1 distances and the *M*1—O1—*M*1 angle with chemical composition are shown in Fig. 1. There are two different trends. The solid circles in the figure represent the extrapolated values for the imaginary $NaInSi_2O_6$ pyroxene [hereafter abbreviated $NaIn(\alpha)$-P_x]. The extrapo-

lated values are 2·190 Å for ⟨*M*1—O1⟩, 3·308 Å for *M*1—*M*1 and 98·0° for *M*1—O1—*M*1, respectively. The real $NaInSi_2O_6$ pyroxene is hereafter abbreviated to NaIn(β)-P_x.

The variations of *M*1—*M*1 distance and *M*1—O1—*M*1 angle with ⟨*M*1—O1⟩ are shown in Fig. 2; *M*1—*M*1 ≃ 2⟨*M*1—O1⟩sin[(*M*1—O1—*M*1)/2]. The solid circles in the figure represent the estimated values for NaIn(α)-P_x. Note that there are two different trends: the Na[In(α),Sc]Si_2O_6 series and the Na[In(β),Sc]Si_2O_6 series.

The pyroxenes used in this study were formed at 6 GPa pressure. However, as mentioned above, the crystal structure of the In100 pyroxene is the same as that of the $NaInSi_2O_6$ pyroxene formed at atmospheric pressure. Furthermore, the two polymorphs of the In40Sc60 pyroxene show that the Na[In(α),Sc]Si_2O_6 pyroxene changes to the Na[In(β),Sc]Si_2O_6 pyroxene by heating at atmospheric pressure. These facts indicate that the Na[In(α),Sc]Si_2O_6 pyroxene is the high-pressure polymorph and the Na[In(β),Sc]Si_2O_6 pyroxene is the low-pressure polymorph.

The phase transition between the two polymorphs may be caused by the geometrical change of the octahedral site. Since *M*1—O1—*M*1 + O1—*M*1—O1 = 180°, the two trends in Figs. 1 and 2 imply that the In(α) ion occupies a less distorted octahedral site, and In(β) ion occupies a more distorted octahedral site.

These physico-chemical and crystal-chemical results suggest that there are two different electronic states (*e.g.* d^{10}, *d*–*s* mixing and/or *d*–*p* mixing states) for the octahedral In^{3+} ions, reflecting pressure and chemical conditions.

Si *tetrahedron*

There are two kinds of bonds in the pyroxene tetrahedron; one is a bridging (br) bond connecting the tetrahedra along the chain, and the other is a nonbridging (nbr) bond, with each tetrahedron having two (br) and two (nbr) bonds. Fig. 3 shows the variations of Si—O3—Si and O3—O3—O3 angles with chemical composition. The Si—O3—Si angle increases with increasing In content, that is, with an increase of the mean radius of the M^{3+} ions. On the other hand, the O3—O3—O3 angle correlates with chemical composition along two different trends: the Na[In(α),Sc]Si_2O_6 pyroxenes and the Na[In(β),Sc]Si_2O_6 pyroxenes. Fig. 4 shows the variations of ⟨Si—O(br)⟩ and ⟨Si—O(nbr)⟩ distances with chemical composition. ⟨Si—O(br)⟩ does not vary significantly with chemical composition. On the other hand, ⟨Si—O(nbr)⟩ correlates with chemical composition in two different ways. ⟨Si—O(nbr)⟩ in Na[In(α),Sc]Si_2O_6 pyroxene decreases with increasing In(α) content. By contrast, ⟨Si—O(nbr)⟩ in Na[In(β),Sc]Si_2O_6 pyroxene does not change with chemical composition.

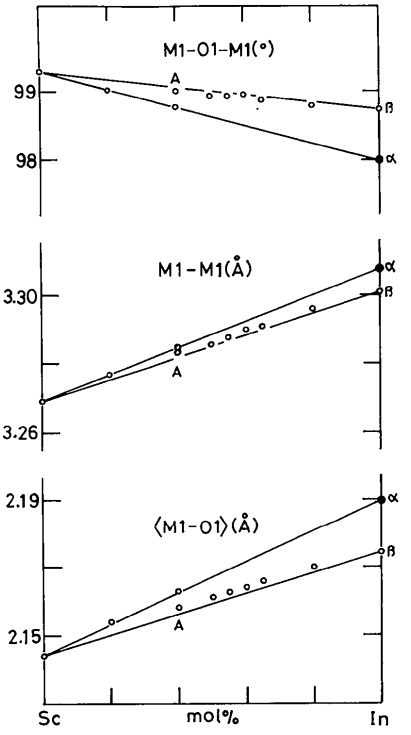

Fig. 1. Variation of *M*1—O1—*M*1 angle, *M*1—*M*1 distance and mean *M*1—O1 distance with chemical composition in Na(In,Sc)Si_2O_6 pyroxenes. Solid circles represent the extrapolated values for NaIn(α)-P_x.

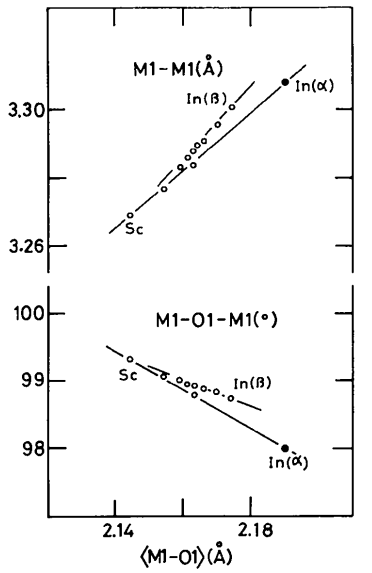

Fig. 2. Variation of *M*1—*M*1 distance and *M*1—O1—*M*1 angle with mean *M*1—O1 distance in Na(In,Sc)Si_2O_6 pyroxenes. Solid circles represent the extrapolated values for NaIn(α)-P_x.

The dependence of Si—O distances on size, electronegativity and electron density of the octahedral M^{3+} ion in $NaM^{3+}Si_2O_6$ pyroxenes was examined by Ohashi (1979, 1981, 1983) and Ohashi, Fujita & Osawa (1982, 1983). Generally, ⟨Si—O⟩ increases with an increase in the radius of the M^{3+} ion. In the Sc–Ti–V–Cr–Al series, the size of the M^{3+} ion affects Si—O(br) and Si—O(nbr) equally. On the other hand, in the In–Fe–Ga series, the size of the M^{3+} ion affects only Si—O(br).

Assuming that the $Na[In(\alpha),Sc]Si_2O_6$ pyroxene belongs to the Sc–Al series, the differences, $d_{br-\Delta}$ and $d_{nbr-\Delta}$, are independent of the size of the M^{3+} ion, where $\Delta = \{\langle Si—O\rangle$ in $Na[In(\alpha),Sc]Si_2O_6\} - \{\langle Si—O\rangle$ in $NaAlSi_2O_6\}$, $d_{br-\Delta} = \langle Si—O(br)\rangle - \Delta$, and $d_{nbr-\Delta} = \langle Si—O(nbr)\rangle - \Delta$. Δ, $d_{br-\Delta}$ and $d_{nbr-\Delta}$ for the $Na[In(\alpha)Sc]Si_2O_6$ pyroxenes are listed in Table 5 and shown in Fig. 5.

The scaled Si—O(br) distance increases and the scaled Si—O(nbr) distance decreases with an increase in the $NaIn(\alpha)Si_2O_6$ component, suggesting that the $In(\alpha)^{3+}$ ion is more electropositive than the Sc^{3+} ion. These changes may be accompanied by expansion of the Si orbitals and by an increases in the π bonding between Si and O(nbr). The solid circles in the figure represent the extrapolated values for $NaIn(\alpha)$-P_x. The extrapolated values are 1·651 Å for $d_{br-\Delta}$ and 1·595 Å for $d_{nbr-\Delta}$.

Table 5. *The differences* (Å), Δ, $d_{br-\Delta}$, $d_{nbr-\Delta}$ *and* $d_{br-2\Delta}$, *in* $Na(In,Sc)Si_2O_6$ *pyroxenes and the mean electronegativity* (χ) *of the octahedral ions*

	Δ*	$d_{br-\Delta}$	$d_{nbr-\Delta}$	$d_{br-2\Delta}$	χ
In100	0·009			1·635	1·7
In80Sc20	0·009			1·634	1·62
In65Sc35	0·008			1·636	1·56
In60Sc40	0·008			1·636	1·54
In55Sc45	0·009			1·635	1·508
In50Sc50	0·008			1·635	1·484
In40Sc60A	0·007			1·637	1·46
In(α)100		1·651†	1·595†		1·18†
In40Sc60	0·006	1·646	1·599		1·252
In20Sc80	0·007	1·645	1·601		1·276
Sc100	0·009	1·644	1·602		1·3

* $\Delta = \langle Si—O\rangle - 1·623$ (Å).
† Extrapolated values.

On the other hand, Si—O distances in $Na[In(\beta),Sc]Si_2O_6$ pyroxenes do not change with composition (Fig. 4). Assuming that $In(\beta)$-P_x belongs to the In–Ga series, the difference, $d_{br-2\Delta}$, and the mean Si—O(nbr) distance are independent of the size of the M^{3+} ion, where $d_{br-2\Delta} = \langle Si—O(br)\rangle - 2\Delta$. Δ and $d_{br-2\Delta}$ are listed in Table 5 and are shown in Fig. 5. In the $Na[In(\beta),Sc]Si_2O_6$ pyroxenes, ⟨Si—O⟩ and the scaled Si—O distances do not change with composition, suggesting that they do not depend on the mean electronegativity of the octahedral ions.

Fig. 6 and Table 6 show the variation of scaled Si—O distance with the electronegativity of the octahedral M^{3+} ion. The solid circles in the figure represent the scaled and extrapolated Si—O distances for the $Na[In(\alpha),Sc]Si_2O_6$ pyroxenes. Assuming that

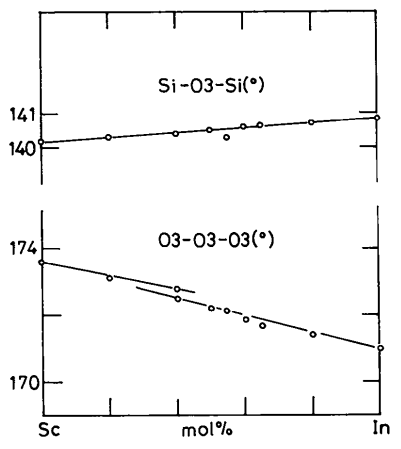

Fig. 3. Variation of Si—O3—Si and O3—O3—O3 angles with chemical composition in $Na(In,Sc)Si_2O_6$ pyroxenes.

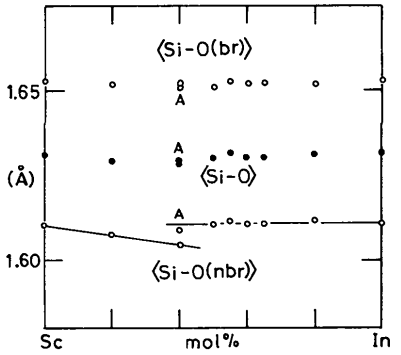

Fig. 4. Si—O distances *versus* chemical composition in $Na(In,Sc)Si_2O_6$ pyroxenes. Open circles represent ⟨Si—O(br)⟩ and ⟨Si—O(nbr)⟩ distances; solid circles represent ⟨Si—O⟩ distances.

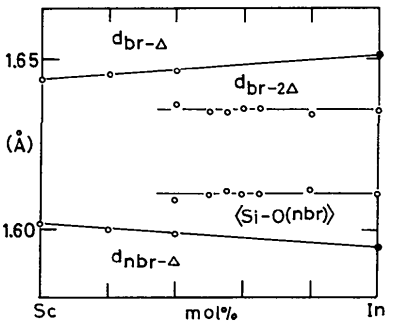

Fig. 5. The differences, $d_{br-\Delta}$, $d_{nbr-\Delta}$ and $d_{br-2\Delta}$, and ⟨Si—O(nbr)⟩ distances *versus* chemical composition in $Na(In,Sc)Si_2O_6$ pyroxenes. Solid circles represent the extrapolated values for $NaIn(\alpha)$-P_x.

$Na[In(\alpha),Sc]Si_2O_6$ pyroxene belongs to the Sc–Al series, the electronegativity of the $In(\alpha)$ is estimated as 1·18 on Pauling's scale.

Ionic radius and electronegativity of indium

The $\langle M^{3+}—O\rangle$ distance in $NaM^{3+}Si_2O_6$ pyroxene is represented by the equation $\langle M^{3+}—O\rangle = 0{\cdot}815r_{M^{3+}} + 1{\cdot}496$ (Å), where $r_{M^{3+}}$ is the effective radius of the M^{3+} ion (Ribbe & Prunier, 1977). The $\langle In—O\rangle$ distance in $NaIn(\alpha)Si_2O_6$ pyroxene is estimated as 2·153 Å from the $\langle(In,Sc)—O\rangle$ distances in $Na[In(\alpha),Sc]Si_2O_6$ pyroxenes, and the $\langle In—O\rangle$ distance in $NaIn(\beta)Si_2O_6$ pyroxene is 2·141 Å. Therefore, the effective ionic radii of $In(\alpha)$ and (β) are 0·805 and 0·791 Å, respectively. These values are nearly the same as the effective ionic radius (r = 0·80 Å) (Shannon, 1976).

On the other hand, there is considerable variation in the electronegativities of the octahedral In^{3+} ions. The electronegativities of $In(\alpha)$ and (β) are estimated as 1·18 and 1·7, respectively. The former is unusually electropositive, and the latter is coincident with the electronegativity calculated from the heat of formation of indium halides (Pauling, 1960; Ohashi, 1987). These variations may be caused by the different electronic structures (*e.g.* d^{10}, *d–s* mixing and *d–p* mixing states) mentioned above.

The $Na(In,Sc)Si_2O_6$ pyroxenes used in this study were formed at 6 GPa pressure. However, as mentioned above, $In(\alpha)$ is the high-pressure-type ion and $In(\beta)$ is the low-pressure-type ion. At high pressure, the In—O distance is short and the crystal field is strong. Therefore, it is expected that the outer ten electrons will occupy the 4*d* orbitals and the screening constant for the d^{10} state will be higher than those for the *d–s* and/or *d–p* mixing states. Thus the unusual electropositive character of $In(\alpha)$ may be caused by the high screening constant for the d^{10} state.

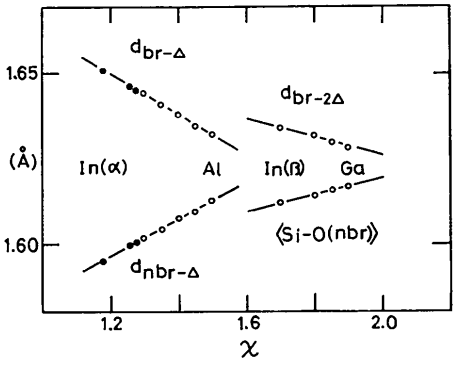

Fig. 6. The differences, $d_{br-\Delta}$, $d_{nbr-\Delta}$ and $d_{br-2\Delta}$, and $\langle$Si—O(nbr)$\rangle$ distance *versus* electronegativity (χ) of the M^{3+} ion for $NaM^{3+}Si_2O_6$ pyroxenes. Solid circles represent the scaled and extrapolated Si—O distances for $Na[In(\alpha),Sc]Si_2O_6$ pyroxenes.

Table 6. *The differences* (Å), Δ, $d_{br-\Delta}$, $d_{nbr-\Delta}$ *and* $d_{br-2\Delta}$, *and* $\langle$Si—O(nbr)$\rangle$ *distances* (Å) *in* $NaM^{3+}Si_2O_6$ *pyroxenes and the electronegativities* (χ) *of the* M^{3+} *ions*

The electronegativities in parentheses are the estimated values; other values from Pauling (1960).

M^{3+}	Δ*	$d_{br-\Delta}$	$d_{nbr-\Delta}$	$d_{br-2\Delta}$	⟨Si—O(nbr)⟩	χ	Ref.
Sc	0·009	1·644	1·602			1·3	(*a*)
Cr	0·001	1·641	1·605			(1·35)†	(*b*)
V	0·001	1·638	1·608			(1·4)†	(*a*)
Ti	0·004	1·635	1·610			(1·45)†	(*c*)
Al	0	1·632	1·613			1·5	(*a*)
In(β)	0·009			1·634	1·612	1·7	(*a*)
Fe	0·005			1·632	1·614	1·8	(*a*)
Mn	0·008			1·630	1·616	(1·85)†	(*d*)
Ga	0·003			1·628	1·617	(1·9)	(*e*)

References: (*a*) Ohashi (1981); (*b*) Ohashi (1983); (*c*) Ohashi, Fujita & Osawa (1982); (*d*) Ohashi, Osawa & Tsukimura (1987); (*e*) Ohashi, Fujita & Osawa (1983).

* Δ is equal to $\langle$Si—O$\rangle$ − 1·623 (Å).

† These values are changeable and increase with an increase in the regularity of the octahedral site (*e.g.* Cr changes from 1·35 to 1·55).

References

CLARK, J. R., APPLEMAN, D. E. & PAPIKE, J. J. (1969). *Mineral. Soc. Am. Spec. Pap.* **2**, 31–50.

Enraf–Nonius (1985). *Structure Determination Package*. Enraf–Nonius, Delft, The Netherlands.

FUKUNAGA, O., YAMAOKA, S., ENDO, T., AKAISHI, M. & KANDA, H. (1979). *High-Pressure Sci. Technol.* **1**, 846–852.

HAWTHORNE, F. C. & GRUNDY, H. D. (1973). *Acta Cryst.* B**29**, 2615–2616.

HAWTHORNE, F. C. & GRUNDY, H. D. (1974). *Acta Cryst.* B**30**, 1882–1884.

OHASHI, H. (1979). *J. Jpn. Assoc. Mineral. Petrol. Econ. Geol.* **74**, 413–416.

OHASHI, H. (1981). *J. Jpn. Assoc. Mineral. Petrol. Econ. Geol.* **76**, 308–311.

OHASHI, H. (1983). *J. Jpn. Assoc. Mineral. Petrol. Econ. Geol.* **78**, 274–280.

OHASHI, H. (1987). *Thermochim. Acta*, **120**, 115–120.

OHASHI, H., FUJITA, T. & OSAWA, T. (1982). *J. Jpn. Assoc. Mineral. Petrol. Econ. Geol.* **77**, 305–309.

OHASHI, H., FUJITA, T. & OSAWA, T. (1983). *J. Jpn. Assoc. Mineral. Petrol. Econ. Geol.* **78**, 159–163.

OHASHI, H., OSAWA, T. & TSUKIMURA, K. (1987). *Acta Cryst.* C**43**, 605–607.

PAULING, L. (1960). *The Nature of the Chemical Bond*, 3rd ed. Ithaca: Cornell Univ. Press.

RIBBE, P. H. & PRUNIER, A. R. (1977). *Am. Mineral.* **62**, 710–720.

SHANNON, R. D. (1976). *Acta Cryst.* A**32**, 751–767.